Applied Physics Letters

Hall effect in the extremely large magnetoresistance semimetal WTe_2

Cite as: Appl. Phys. Lett. **107**, 182411 (2015); https://doi.org/10.1063/1.4935240
Submitted: 04 September 2015 • Accepted: 25 October 2015 • Published Online: 06 November 2015

Yongkang Luo, H. Li, Y. M. Dai, et al.

Hall effect in the extremely large magnetoresistance semimetal WTe_2

Yongkang Luo,[1,a),b)] H. Li,[2,b)] Y. M. Dai,[1] H. Miao,[2] Y. G. Shi,[2] H. Ding,[2,3] A. J. Taylor,[1] D. A. Yarotski,[1] R. P. Prasankumar,[1] and J. D. Thompson[1]
[1]*Los Alamos National Laboratory, Los Alamos, New Mexico 87545, USA*
[2]*Beijing National Laboratory for Condensed Matter Physics, Institute of Physics, Chinese Academy of Science, Beijing 100190, China*
[3]*Collaborative Innovation Center of Quantum Matter, Beijing 100084, China*

(Received 4 September 2015; accepted 25 October 2015; published online 6 November 2015)

We systematically measured the Hall effect in the extremely large magnetoresistance semimetal WTe_2. By carefully fitting the Hall resistivity to a two-band model, the temperature dependencies of the carrier density and mobility for both electron- and hole-type carriers were determined. We observed a sudden increase in the hole density below ~160 K, which is likely associated with the temperature-induced Lifshitz transition reported by a previous photoemission study. In addition, a more pronounced reduction in electron density occurs below 50 K, giving rise to comparable electron and hole densities at low temperature. Our observations indicate a possible electronic structure change below 50 K, which might be the direct driving force of the electron-hole "compensation" and the extremely large magnetoresistance as well. Numerical simulations imply that this material is unlikely to be a perfectly compensated system. © *2015 AIP Publishing LLC*.
[http://dx.doi.org/10.1063/1.4935240]

The past few years have witnessed the discovery of a series of new non-magnetic compounds with very large magnetoresistance (MR),[1–5] even much larger than those traditional giant MR in thin film metals[6] and colossal MR in Cr-based chalcogenide spinels[7] and Mn-based perovskites.[8] With many potential applications in magnetic field sensors, read heads, random access memories, and galvanic isolators,[9] these newly discovered extremely large MR (XMR) materials have attracted enormous interest. Several mechanisms have been proposed as the origin of the XMR in these materials, e.g., (i) topological protection from backward scattering mechanism and (ii) electron-hole compensation mechanism. The former has been realized in Dirac semimetals like Cd_3As_2[4,10] and Weyl semimetals like *TmPn* (where *Tm* = Ta or Nb, and *Pn* = As or P),[5,11–15] while the latter stems from a multi-band effect:[16] although no net current flows in the **y**-direction, currents in the **y**-direction carried by a particular type of carrier may be non-zero. These transverse currents experience a Lorentz force that is antiparallel to the **x**-direction. This backflow of carriers provides an important source of magnetoresistance, which is most pronounced in semimetals like Bi[17] and graphite[18] where electrons and holes are compensated.

Recently, the observation of XMR in high-purity WTe_2 has triggered great enthusiasm.[3] Angle-resolved photoemission spectroscopy (ARPES) studies have revealed the coexistence of multiple electron and hole Fermi surfaces (FSs) with the total size of electron pockets close to that of hole pockets,[19–21] which is further supported by Shubnikov-de Hass (SdH) quantum oscillation[22,23] measurements, reminiscent of the electron-hole compensation mechanism for WTe_2. Furthermore, ARPES measurements also manifested a temperature-induced Lifshitz transition at about 160 K, above which all the hole bands sink below the Fermi level.[21] This raises the possibility that the temperature-induced Lifshitz transition may be the driving force for the electron-hole compensation as well as the XMR at low temperatures. On the other hand, a more recent transport study reported that the mass anisotropy grows sharply below ~50 K,[24] closely following the temperature dependence of the MR. This mass anisotropy enhancement has been associated with a change in the electronic structure that is believed to play a key role in turning on the XMR in WTe_2. Direct evidence for these views may be produced by a thorough investigation into the temperature dependence of the carrier density that can be determined by Hall effect measurements.

In this letter, we performed systematic measurements of electrical transport properties (ρ_{xx} and ρ_{yx}) on high-quality WTe_2 single crystals. A careful fitting of $\rho_{yx}(B)$ to a two-band model yields the temperature dependencies of the carrier density and mobility for both electron- and hole-type of carriers. The signature of the temperature-induced Lifshitz transition at ~160 K was observed. In addition, the electron carrier density significantly drops below 50 K, leading to a *nearly* compensated situation at low temperature which is probably the cause of the XMR. These experiments pose an interesting "paradox" between a quadratic-law for $\rho_{xx}(B)$ and a non-linear $\rho_{yx}(B)$. Further numerical simulations suggest that WTe_2 is unlikely to be a perfectly compensated system. Our results reveal the mechanism of the XMR in WTe_2, shedding light on this peculiar material with great potential for electronic device applications.

The experimental details and sample characterization have been addressed in the supplementary material.[25] The main panel of Fig. 1(a) shows the temperature dependent resistivity of WTe_2 measured without an external magnetic field. Our sample is characterized by a huge residual resistance ratio [RRR $\equiv R(300\,\mathrm{K})/R(1.3\,\mathrm{K}) = 1463$], which is among the highest reported.[3,21–23,26] In Figs. 1(b) and 1(c),

[a)]Electronic address: ykluo@lanl.gov
[b)]Y. Luo and H. Li contributed equally to this work.

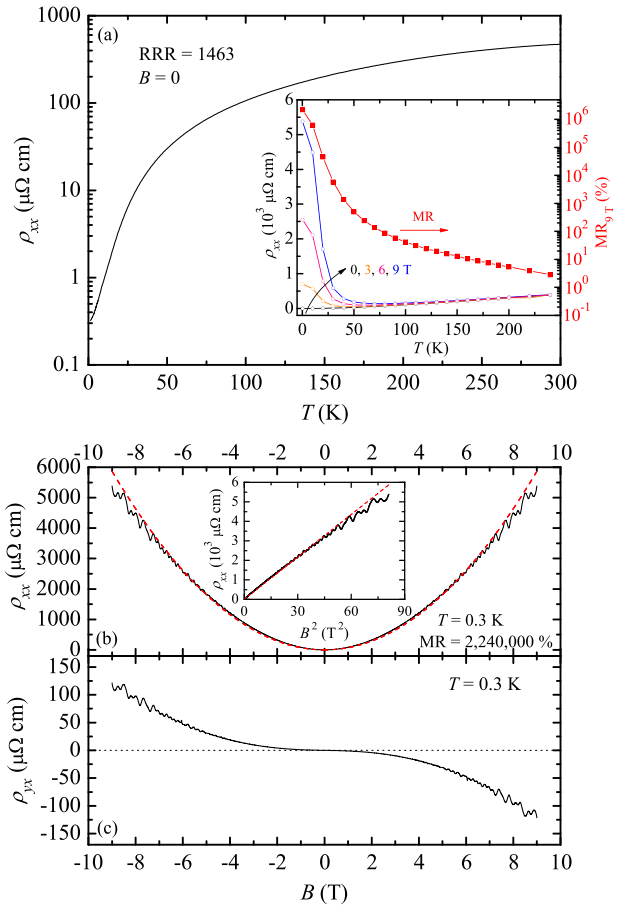

FIG. 1. (a) Temperature dependence of the resistivity $\rho_{xx}(T)$ of WTe_2 in the absence of a magnetic field. The inset shows a comparison of $\rho_{xx}(T)$ at $B = 0$, 3, 6, and 9 T (left axis), and $\%MR_{9T} \equiv 100 \times [\rho_{xx}(9\,T) - \rho_{xx}(0)]/\rho_{xx}(0)$ (right axis). (b) and (c) Display the field dependencies of ρ_{xx} and ρ_{yx} at 0.3 K, respectively. The inset of (b) shows $\rho_{xx}(B)$ plotted in the B^2 scale with the red-dashed line as a linear guide to the eyes.

we, respectively, present ρ_{xx} and ρ_{yx} at $T = 0.3$ K as a function of magnetic field B. The field dependence of ρ_{xx} roughly follows a quadratic behavior [red-dashed line in Fig. 1(b)] without any trend of saturation.[3] The resulting extremely large magnetoresistance $\%MR \equiv 100 \times [\rho_{xx}(B) - \rho_{xx}(0)]/\rho_{xx}(0)$ reaches 2 240 000% at 9 T, comparable with the values in previous reports.[3,21–23,26] The large magnitudes of RRR and MR guarantee the high quality of our WTe_2 single crystal. Another important feature of the magneto-transport properties in WTe_2 is the large SdH quantum oscillations, observed in both $\rho_{xx}(B)$ [Fig. 1(b)] and $\rho_{yx}(B)$ [Fig. 1(c)]. By taking the Fast Fourier Transform of the oscillatory part $\Delta\rho_{xx} = \rho_{xx} - \langle\rho_{xx}\rangle$ (where $\langle\rho_{xx}\rangle$ is the non-oscillatory background), we derived the extremal cross-sectional areas S_F of the FSs that are similar to Zhu *et al.*[22] The supplementary material[25] provides more details about SdH oscillations.

Figures 2(a) and 2(b) depict the field dependence of ρ_{yx} at selected temperatures ranging from 0.3 K to 240 K. It is evident that for all temperatures, ρ_{yx} is negative, manifesting an electron-dominant characteristic. We also note that ρ_{yx} is not a linear function of B. This non-linearity of $\rho_{yx}(B)$ becomes more pronounced at low temperature, and is also reflected in the temperature dependent Hall coefficient R_H as shown in Fig. 2(c). The solid symbols in Fig. 2(c) signify $R_H(9\,T)$ defined by ρ_{yx}/B at $B = 9$ T, and the open symbols stand for $R_H(0)$ determined from the initial slope of $\rho_{yx}(B)$ near $B = 0$. At high temperatures, the two curves more or less overlap, whereas they apparently diverge below ~160 K. This divergence is more significant below 20 K where $R_H(9\,T)$ dramatically decreases but $R_H(0)$, on the contrary, starts to increase. All these arise from the multi-band effect in this material. In fact, according to the recent band structure calculations,[3] ARPES,[21] and SdH[22] results, the FS of WTe_2 at low temperatures consists of two electron-like sheets and two hole-like sheets on each side of the **Γ**–**X** line in the 1st Brillouin zone.

For simplicity, here we adopt a two-band model with one electron-and one hole-bands. This model has been successfully used to describe the Hall effect in multi-band iron-pnictides,[27,28] and we will see that it is sufficient to explain the Hall effect in the full temperature range. The total conductivity tensor $\boldsymbol{\sigma}$ is conveniently expressed in the complex representation[3]

$$\boldsymbol{\sigma} = e\left[\frac{n_e\mu_e}{1 + i\mu_e B} + \frac{n_h\mu_h}{1 - i\mu_h B}\right], \tag{1}$$

where n and μ are carrier density and mobility, and the subscript e (or h) denotes electron (or hole). Converting this equation into the resistivity tensor ($\boldsymbol{\rho} = \boldsymbol{\sigma}^{-1}$), ρ_{xx} and $\rho_{xy}(=-\rho_{yx})$ are the real and imaginary parts of $\boldsymbol{\rho}$, respectively, i.e.,

$$\rho_{xx}(B) = \mathrm{Re}(\boldsymbol{\rho}) = \frac{1}{e}\frac{(n_h\mu_h + n_e\mu_e) + (n_h\mu_e + n_e\mu_h)\mu_h\mu_e B^2}{(n_h\mu_h + n_e\mu_e)^2 + (n_h - n_e)^2\mu_h^2\mu_e^2 B^2}, \tag{2a}$$

$$\rho_{yx}(B) = -\mathrm{Im}(\boldsymbol{\rho}) = \frac{B}{e}\frac{\left(n_h\mu_h^2 - n_e\mu_e^2\right) + (n_h - n_e)\mu_h^2\mu_e^2 B^2}{(n_h\mu_h + n_e\mu_e)^2 + (n_h - n_e)^2\mu_h^2\mu_e^2 B^2}. \tag{2b}$$

All the $\rho_{yx}(B)$ data measured at different temperatures can be well fitted to Eq. (2b), with n_e, n_h, μ_e, and μ_h being fitting parameters. Some representative results are displayed in Figs. 2(a) and 2(b). The fitting derives the temperature dependencies of carrier density and mobility for both electron- and hole-type carriers, shown in Figs. 2(d) and 2(e), respectively. An important feature of $n_h(T)$ is that it increases abruptly below ~160 K. At 170 K, $n_h = 0.41 \times 10^{19}$ cm^{-3}. It increases to 0.86×10^{19} cm^{-3} at 140 K, more than twice of the value at 170 K. Temperature dependent ARPES measurements have pointed out that a temperature-induced Lifshitz transition is likely to occur at about 160 K, below which the hole pockets appear.[21] The observed upturn of $R_H(T)$ [see inset to Fig. 2(c)] and the enhancement of $n_h(T)$ below this critical temperature are consistent with the temperature-induced Lifshitz transition. Furthermore, we noticed that $n_e(T)$ decreases drastically below 50 K. More interestingly, $n_e(T)$ and $n_h(T)$ tend to be comparable at low temperature. This is better seen in the ratio n_h/n_e shown in the inset of Fig. 2(d). In particular, at 0.3 K, $n_e = 8.82 \times 10^{19}$ cm^{-3} and $n_h = 7.64 \times 10^{19}$ cm^{-3}. These values are very close to the carrier densities determined from SdH measurements[22] (see also the

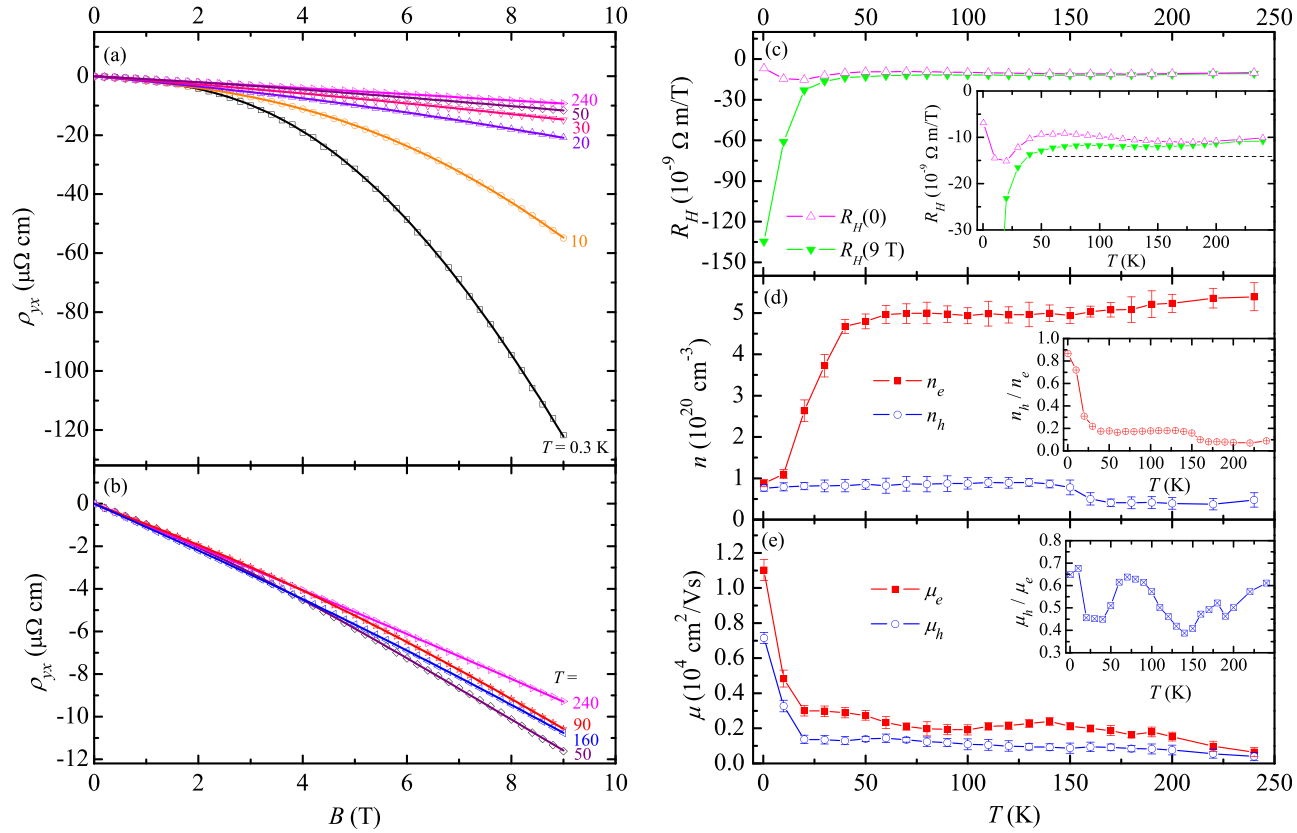

FIG. 2. (a) and (b) Field dependencies of the Hall resistivity at various temperatures. The curve for 0.3 K is the non-oscillating background $\langle \rho_{yx} \rangle$. The open symbols are experimental data, while the solid lines running through the data are numerical fitting to a two-band model Eq. (2b). (c) Hall coefficient R_H as a function of T. The solid symbols signify the R_H defined by ρ_{yx}/B at $B = 9$ T, while the open symbols stand for R_H determined from the initial slope of $\rho_{yx}(B)$ at $B \to 0$. The dashed line in the inset is a guide line to eyes. (d) and (e) Display the temperature dependent carrier density and mobility, respectively. The insets to (d) and (e) show the plot of n_h/n_e and μ_h/μ_e versus T.

supplementary material). Furthermore, $T = 50$ K is also the characteristic temperature below which the magnetoresistance starts to increase dramatically, see the inset of Fig. 1(b). Thermopower measurements also exhibit a sign change from being positive to negative upon cooling through 50 K.[21,29] Our recent ultrafast optical pump-probe spectroscopic measurements also revealed that the timescale governing electron-hole recombination, which is sensitive to the electronic structure, shows a strong anomaly at ~50 K.[30] All these experimental results suggest a potential electronic structure change below 50 K, which is likely the direct driving mechanism of the electron-hole "compensation" and the XMR at low temperature as well. Since no systematic temperature dependent ARPES measurements have been done for temperatures below 50 K, the nature of this electronic structure change remains an open question that needs to be clarified in the future.

Finally, we realized an interesting "paradox" between the behaviors of $\rho_{xx}(B)$ and $\rho_{yx}(B)$. According to Eq. (2a), the condition for $\rho_{xx}(B)$ to increase as B^2 is $n_e = n_h$, which is the case that electrons and holes are *perfectly* compensated by each other.[3] However, this inevitably leads to linearity of $\rho_{yx}(B)$ [see Eq. (2b)], which is apparently at odds with the experimental data shown in Fig. 2. This paradox cannot be reconciled by tuning the carrier mobilities or introducing additional bands, but can only be resolved by slightly unbalancing n_h and n_e.

To better clarify this, we performed numerical simulations as displayed in Fig. 3. All quantities depicted here are in arbitrary units. In Figs. 3(a) and 3(b), we calculated $\rho_{xx}(B)$ and $\rho_{yx}(B)$ based on the two-band model Eq. (1). The black curves A signify the perfect compensation condition, with the parameters $n_e = 1.00$, $n_h = 1.00$, $\mu_e = 1.00$, and $\mu_h = 0.65$, and indeed, we obtained quadratic $\rho_{xx}(B)$ and linear $\rho_{yx}(B)$. Slightly decreasing n_h, e.g., 0.92, we found that $\rho_{xx}(B)$ weakly deviates from the quadratic-law and meanwhile $\rho_{yx}(B)$ is strongly non-linear (see curve B), which is qualitatively similar to the experimental data shown in Figs. 1(b) and 1(c). As a comparison, we also show in Figs. 3(c) and 3(d) the simulations based on a three-band model. The total conductivity tensor now becomes

$$\boldsymbol{\sigma} = e\left[\frac{n_e\mu_e}{1+i\mu_e B} + \frac{n'_e\mu'_e}{1+i\mu'_e B} + \frac{n_h\mu_h}{1-i\mu_h B}\right], \qquad (3)$$

and the condition for a perfect electron-hole compensation changes to $n_e + n'_e = n_h$. Nevertheless, the compensation condition still leads to the aforementioned paradox. To note, the situation cannot be improved by introducing a fourth band or even more bands (data not shown). All these suggest that WTe_2 is not a purely compensated system, whereas we should admit that a slight mismatch between n_e and n_h does not strongly affect the XMR [Curves B and C in Fig. 3(a)].

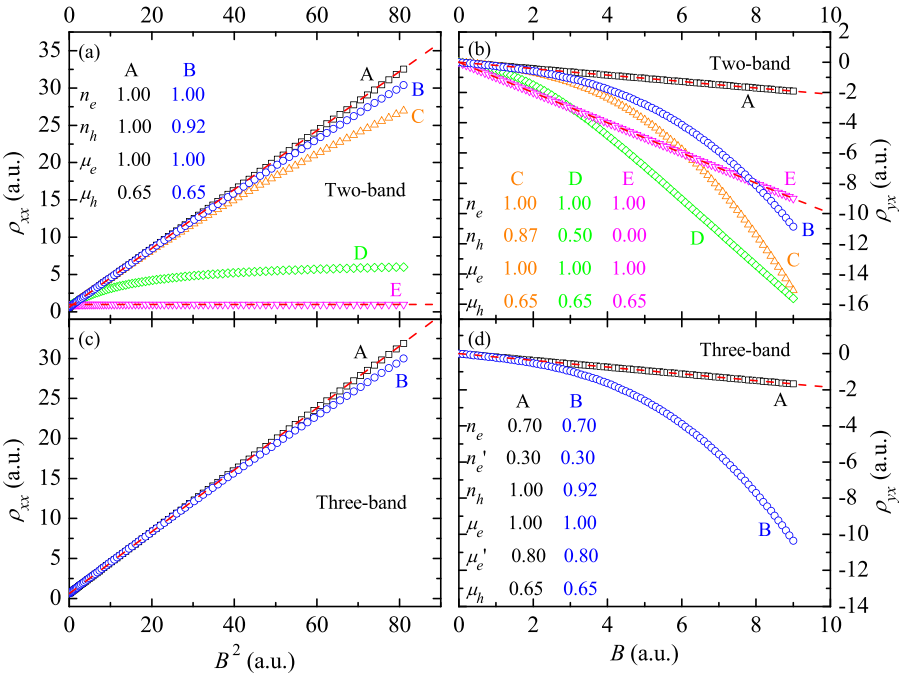

FIG. 3. Numerical simulations of $\rho_{xx}(B)$ (left panels) and $\rho_{yx}(B)$ (right panels). The parameters are listed in panels (a), (b), and (d). The red dashed lines are the linear guides to the eyes. (a) and (b) are calculated with a two-band model. (c) and (d) are calculated with a three-band model.

XMR disappears when n_e and n_h are severely unbalanced, seeing the curves D and E in Fig. 3(a).

To summarize, we analysed the Hall effect in the extremely large magnetoresistance semimetal WTe_2 within a two-band model, and derived the temperature dependencies of the carrier density and mobility for both electron- and hole-type carriers. Below ~160 K, the hole carrier density abruptly increases, consistent with a temperature-induced Lifshitz transition observed by a previous ARPES study. Moreover, the electron-type carrier density decreases sharply below 50 K, and at low temperature, the carrier densities of electrons and holes become comparable. Our results indicate a possible electronic structure change at about 50 K, which is likely to drive the electron-hole "compensation" that promotes the extremely large magnetoresistance. We also performed numerical simulations of $\rho_{xx}(B)$ and $\rho_{yx}(B)$ based on multi-band models, and our calculations suggest that this material is unlikely to be a perfectly compensated system.

We thank John Bowlan, Pamela Bowlan, Brian McFarland, and F. Ronning for insightful discussions. Work at Los Alamos was performed under the auspices of the U.S. Department of Energy, Division of Materials Science and Engineering, Center for Intergrated Nanotechnologies, and UC Office of the President under the UC Lab Fees Research Program. Work at IOP CAS was supported by the Strategic Priority Research Program (B) of the Chinese Academy of Sciences (Grant No. XDB07020100) and the National Natural Science Foundation of China (Nos. 11274367 and 11474330). Y. Luo acknowledges a Director's Postdoctoral Fellowship supported through the LANL LDRD program.

[1]E. Mun, H. Ko, G. J. Miller, G. D. Samolyuk, S. L. Bud'ko, and P. C. Canfield, Phys. Rev. B **85**, 035135 (2012).
[2]K. Wang, D. Graf, L. Li, L. Wang, and C. Petrovic, Sci. Rep. **4**, 07328 (2014).
[3]M. N. Ali, J. Xiong, S. Flynn, J. Tao, Q. D. Gibson, L. M. Schoop, T. Liang, N. Haldolaarachchige, M. Hirschberger, N. P. Ong, and R. J. Cava, Nature **514**, 205 (2014).
[4]T. Liang, Q. Gibson, M. N. Ali, M. Liu, R. J. Cava, and N. P. Ong, Nat. Mater. **14**, 280 (2015).
[5]H. Weng, C. Fang, Z. Fang, B. A. Bernevig, and X. Dai, Phys. Rev. X **5**, 011029 (2015).
[6]W. F. Egelhoff, T. Ha, R. D. K. Misra, Y. Kadmon, J. Nir, C. J. Powell, M. D. Stiles, R. D. McMichael, C. Lin, J. M. Sivertsen, J. H. Judy, K. Takano, A. E. Berkowitz, T. C. Anthony, and J. A. Brug, J. Appl. Phys. **78**, 273 (1995).
[7]A. P. Ramirez, R. J. Cava, and J. Krajewski, Nature **386**, 156 (1997).
[8]S. Jin, M. McCormack, T. H. Tiefel, and R. Ramesh, J. Appl. Phys. **76**, 6929 (1994).
[9]J. M. Daughton, J. Magn. Magn. Mater. **192**, 334 (1999).
[10]Y. Zhao, H. Liu, C. Zhang, H. Wang, J. Wang, Z. Lin, Y. Xing, H. Lu, J. Liu, Y. Wang, S. M. Brombosz, Z. Xiao, S. Jia, X. C. Xie, and J. Wang, Phys. Rev. X **5**, 031037 (2015).
[11]B. Q. Lv, H. M. Weng, B. B. Fu, X. P. Wang, H. Miao, J. Ma, P. Richard, X. C. Huang, L. X. Zhao, G. F. Chen, Z. Fang, X. Dai, T. Qian, and H. Ding, Phys. Rev. X **5**, 031013 (2015).
[12]C. Shekhar, A. K. Nayak, Y. Sun, M. Schmidt, M. Nicklas, I. Leermakers, U. Zeitler, Y. Skourski, J. Wosnitza, Z. Liu, Y. Chen, W. Schnelle, H. Borrmann, Y. Grin, C. Felser, and B. Yan, Nat. Phys. **11**, 645 (2015).
[13]N. J. Ghimire, Y. Luo, M. Neupane, D. J. Williams, E. D. Bauer, and F. Ronning, J. Phys.: Condens. Matter **27**, 152201 (2015).
[14]Y. Luo, N. J. Ghimire, M. Wartenbe, M. Neupane, R. D. McDonald, E. D. Bauer, J. D. Thompson, and F. Ronning, e-print arXiv:1506.01751.
[15]C. Shekhar, F. Arnold, S.-C. Wu, Y. Sun, M. Schmidt, N. Kumar, A. G. Grushin, J. H. Bardarson, R. Donizeth dos Reis, M. Naumann, M. Baenitz, H. Borrmann, M. Nicklas, E. Hassinger, C. Felser, and B. Yan, e-print arXiv:1506.06577.
[16]J. Singleton, *Band Theory and Electronic Properties of Solids* (Oxford University Press, 2001).
[17]P. B. Alers and R. T. Webber, Phys. Rev. **91**, 1060 (1953).
[18]X. Du, S.-W. Tsai, D. L. Maslov, and A. F. Hebard, Phys. Rev. Lett. **94**, 166601 (2005).
[19]I. Pletikosić, M. N. Ali, A. V. Fedorov, R. J. Cava, and T. Valla, Phys. Rev. Lett. **113**, 216601 (2014).
[20]J. Jiang, F. Tang, X. C. Pan, H. M. Liu, X. H. Niu, Y. X. Wang, D. F. Xu, H. F. Yang, B. P. Xie, F. Q. Song, X. G. Wan, and D. L. Feng, Phys. Rev. Lett. **115**, 166601 (2015).
[21]Y. Wu, N. H. Jo, M. Ochi, L. Huang, D. Mou, S. L. Bud'ko, P. C. Canfield, N. Trivedi, R. Arita, and A. Kaminski, Phys. Rev. Lett. **115**, 166602 (2015).
[22]Z. Zhu, X. Lin, J. Liu, B. Fauqué, Q. Tao, C. Yang, Y. Shi, and K. Behnia, Phys. Rev. Lett. **114**, 176601 (2015).
[23]P. L. Cai, J. Hu, L. P. He, J. Pan, X. C. Hong, Z. Zhang, J. Zhang, J. Wei, Z. Q. Mao, and S. Y. Li, Phys. Rev. Lett. **115**, 057202 (2015).

[24]L. R. Thoutam, Y. L. Wang, Z. L. Xiao, S. Das, A. Luican-Mayer, R. Divan, G. W. Crabtree, and W. K. Kwok, Phys. Rev. Lett. **115**, 046602 (2015).
[25]See supplementary material at http://dx.doi.org/10.1063/1.4935240 for structural information, sample characterization, and SdH oscillation analysis.
[26]Y. Zhao, H. Liu, J. Yan, W. An, J. Liu, X. Zhang, H. Wang, Y. Liu, H. Jiang, Q. Li, Y. Wang, X.-Z. Li, D. Mandrus, X. C. Xie, M. Pan, and J. Wang, Phys. Rev. B **92**, 041104 (2015).
[27]F. Rullier-Albenque, D. Colson, A. Forget, and H. Alloul, Phys. Rev. Lett. **103**, 057001 (2009).
[28]F. Rullier-Albenque, D. Colson, A. Forget, P. Thuéry, and S. Poissonnet, Phys. Rev. B **81**, 224503 (2010).
[29]S. Kabashima, J. Phys. Soc. Jpn. **21**, 945 (1966).
[30]Y. M. Dai, J. Bowlan, H. Li, H. Miao, S. F. Wu, W. D. Kong, Y. G. Shi, S. A. Trugman, J.-X. Zhu, H. Ding, A. J. Taylor, D. A. Yarotski, and R. P. Prasankumar, Phys. Rev. B **92**, 161104 (2015).